

# Planarization-Induced Activation Wavelength Red-Shift and Thermal Half-Life Acceleration in Hydrazone Photoswitches

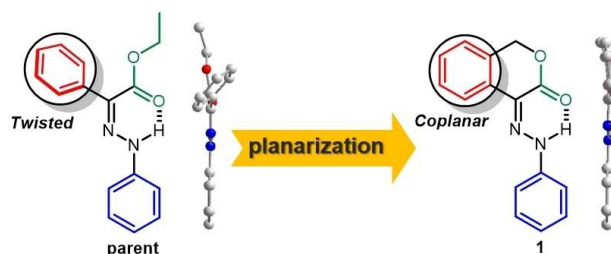
Baihao Shao and Ivan Aprahamian\*<sup>[a]</sup>

The optimization and modulation of the properties of photochromic compounds, such as their activation wavelengths and thermal relaxation half-lives ( $\tau_{1/2}$ ), are essential for their adaptation in various applications. In this work, we studied the effect of co-planarization of the rotary fragment of two photochromic hydrazones with the core of the molecule on their switching properties. The *Z* and *E* isomers of both compounds exhibit red-shifted absorption bands relative to their twisted versions, allowing for their photoswitching using longer wavelengths of light. Additionally, the thermal half-lives of both hydrazones are drastically shortened from hundreds of years to days.

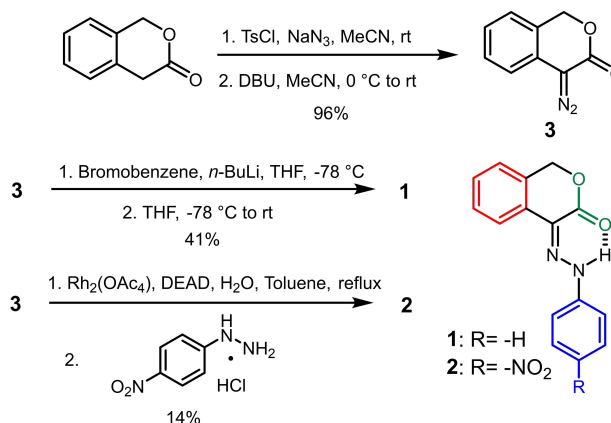
Photochromic compounds<sup>[1]</sup> that undergo reversible *E/Z* isomerization<sup>[2]</sup> or cyclization/ring-opening reactions,<sup>[3]</sup> are indispensable building blocks for the development of light-powered molecular motors and machines,<sup>[4]</sup> responsive nanoparticles and surfaces,<sup>[5]</sup> and switchable drugs (i.e., photopharmacology),<sup>[6]</sup> among others. For such applications, red shifting the activation wavelengths and modulating the thermal relaxation rates of the photoswitches are key components in the optimization of their properties. The former allows for the use of low energy light during switching thus enabling deeper tissue-penetration while lowering phototoxicity.<sup>[7]</sup> The latter property enables the kinetic trapping of the less stable isomer (if it is slow enough)<sup>[8]</sup> or the instantaneous thermal reversion of the photoreaction (if it is made fast),<sup>[9]</sup> thus defining what the photoswitches can be used for. The development of novel strategies that can help in modulating these properties in known systems, will contribute to the integration of photoswitches into diverse applications, in addition to opening the way for new functions and possibilities.<sup>[10]</sup>

Our interest in hydrazone-based materials<sup>[11]</sup> recently resulted in the development of a new family of bistable

hydrazone photoswitches ( $\tau_{1/2}$  of up to 5,300 years).<sup>[12]</sup> Structure-property analyses of the hydrazones led us to the observation that they adopt a uniform molecular geometry (based on their crystal structures) in which the rotor ring (red) is twisted out of the plane of the hydrazone core (Scheme 1).<sup>[13]</sup> This structural property explains why functionalizing the rotor ring with electron donating or withdrawing groups (EDG and EWG, respectively) has a lesser effect on the hydrazones' photophysical properties than derivatizing the stator ring (blue). We hypothesized that enforcing co-planarity on the entire molecule will enhance the conjugation in the hydrazone and thus red-shift its isomerization wavelengths. To this end, we synthesized two hydrazones (1 and 2; Scheme 2) where the rotary ring is linked with the ester group forming an isochromanone-like structure. As expected, compound 1 shows a ~30 nm red shift for both the *E* and *Z* isomers relative to its uncyclized version (**parent**), whilst a further ~20 nm red shift was measured for 2. Moreover, we found that the thermal



Scheme 1. Design of the planar hydrazone, and the side-view crystal structures of the **parent** compound and 1.



Scheme 2. Synthesis of hydrazones 1 and 2.

[a] B. Shao, Prof. Dr. I. Aprahamian  
Department of Chemistry, Dartmouth College, 6128 Burke Laboratory  
Hanover, New Hampshire, 03755 (USA)  
E-mail: ivan.aprahamian@dartmouth.edu

Supporting information for this article is available on the WWW under  
<https://doi.org/10.1002/open.201900340>

An invited contribution to a Special Collection dedicated to Functional Supramolecular Systems

© 2020 The Authors. Published by Wiley-VCH Verlag GmbH & Co. KGaA. This is an open access article under the terms of the Creative Commons Attribution Non-Commercial License, which permits use, distribution and reproduction in any medium, provided the original work is properly cited and is not used for commercial purposes.

relaxation half-lives of both **1** and **2** were accelerated by 4 orders of magnitude (i.e.,  $\tau_{1/2}$  is days and not years).

Compound **1** was synthesized in a straightforward manner (41% yield) by reacting 4-diazoisochroman-3-one (**3**) with freshly prepared phenyllithium in THF (Scheme 2). We previously found<sup>[13]</sup> that having a *para*-nitro substituent at the stator phenyl ring extends the conjugation in the system, resulting in a red-shift in the absorption spectra relative to the unsubstituted hydrazone, and hence we synthesized hydrazone **2** as well. The switch was obtained by reacting the keto ester derivative of **3**<sup>[14]</sup> with (4-nitrophenyl) hydrazine hydrochloride (14% yield). The intermediates and final products were fully characterized using NMR spectroscopy (Figures S1-6), mass spectrometry, and X-ray crystallography (**1**; Figure S21). The N–H protons of **1** and **2** resonate at 12.71 and 12.83 ppm, respectively, indicating that the cyclization does not change the typical H-bond present in the hydrazone switches.

The characteristic H-bonded structure (N–H...O=C, 2.64 Å, 130.27°)<sup>15</sup> is also validated in the crystal structure of 1-Z. The compound has two different packing modes in the crystal, which can be differentiated by the centroid-to-centroid distance between the rotor and stator phenyl rings (Figure 1a). The loosely packed one features a distance of 4.06 Å, while a shorter distance of 3.87 Å was found in the other. Moreover, the X-ray crystallographic analysis offers a more straightforward view on the planarization of the rotary fragment. The dihedral angle between the two planes, where the rotary ring and the hydrazone backbone intersect in the **parent** switch was measured to be 43.5° (Figure 1b), which is a typical value for the hydrazone photoswitches we have developed so far. In **1** on the other hand the dihedral angle in the tighter packed unit is 14.9° (Figure 1c) and is slightly smaller in the looser

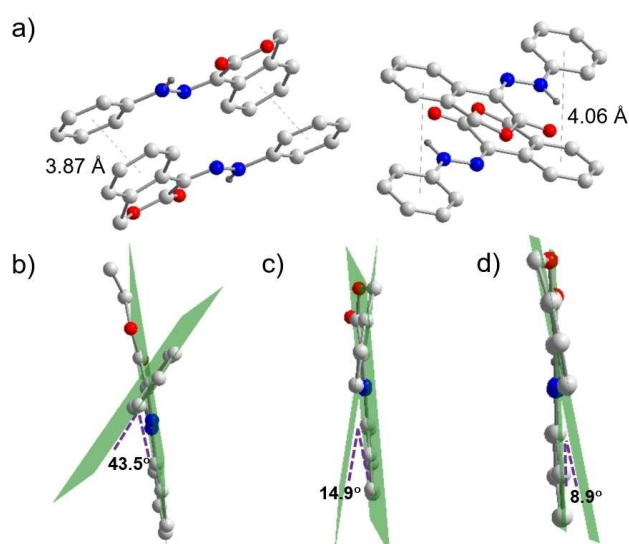


**Figure 1.** a) The two packing modes (centroid-to-centroid distances of 3.87 and 4.06 Å are shown) present in the crystal structure of 1-Z; The dihedral angles between the rotor ring and hydrazone backbone in the b) parent, c) tightly packed 1-Z (left) and d) loosely packed 1-Z (right) are shown (C–H protons are omitted for clarity).

packed one (8.9°; Figure 1d). In both cases the number is much smaller than 43.5°, verifying that the rotary ring becomes less twisted relative to the hydrazone core upon cyclization.

We first studied the photophysical and photochemical properties of hydrazones **1** and **2** using UV/Vis spectroscopy. The spectral data of the pure *E* isomers (> 99%) were difficult to determine experimentally, and hence were extrapolated following a previously reported method.<sup>[13]</sup> The absorption band of an equilibrated solution (toluene; dark) of 1-Z is bathochromically shifted by 31 nm relative to that of the uncyclized **parent** hydrazone, with an absorption maximum ( $\lambda_{\max}$ ) of 398 nm ( $\epsilon=27800 \text{ M}^{-1}\text{cm}^{-1}$ ; Figure 2b). Upon irradiation with 442 nm light, a new band at 369 nm appears (Figure 2b), which was used to determine the absorption maximum of pure *E* to be 366 nm ( $\epsilon=22500 \text{ M}^{-1}\text{cm}^{-1}$ ; Figure S9). The *E* band is again shifted by 32 nm, implying that the enhanced conjugation is also retained in the less rigid (i.e., no intramolecular H-bond) *E* form. The reverse *E*→*Z* photoisomerization can be initiated using 365 nm light, and the switching process between the two isomers can be cycled multiple times with minimal photofatigue by alternating the irradiation wavelength between 442 and 365 nm (Figure S11). As hypothesized, the absorption bands of the nitro-substituted compound **2** (*Z*:  $\lambda_{\max}=415 \text{ nm}$  and  $\epsilon=38300 \text{ M}^{-1}\text{cm}^{-1}$ ; *E*:  $\lambda_{\max}=384 \text{ nm}$  and  $\epsilon=33400 \text{ M}^{-1}\text{cm}^{-1}$ ; Figure 2d and Figure S10) are red-shifted compared to **1**. The *Z/E* isomerization between 2-Z and 2-E can be induced by 442 and 375 nm light sources, and multiple switching cycles (10 tried) show no signs of fatigue (Figure S12).

We next studied the photoswitching efficiency of **1** and **2** using NMR spectroscopy. Irradiation of a toluene solution of **1** or **2** (> 99% *Z*) with 442 nm light induces *Z*→*E* photoisomerization, yielding an *E*-rich photostationary state (PSS) of 86 and 88% *E* (Figures S7-8), respectively, with quantum yields ( $\Phi$ ) of  $5.8 \pm 0.1\%$  (**1**) and  $2.6 \pm 0.1\%$  (**2**). The reverse *E*→*Z* photo-switching of **1** and **2** (Figures S7-8) can be triggered by 365 and 375 nm light sources, respectively, and yields PSS<sub>365</sub> consisting

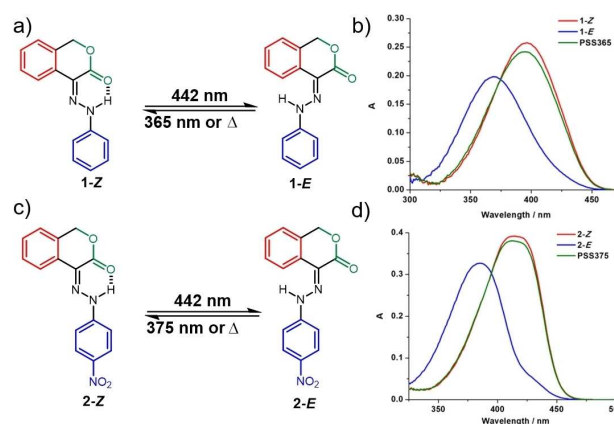
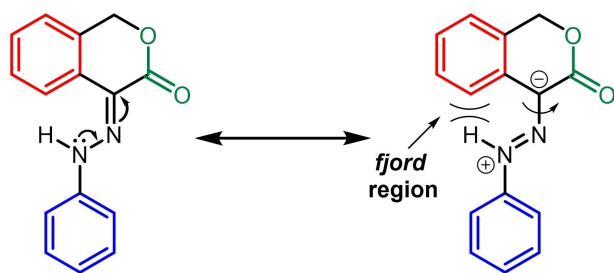


**Figure 2.** a) *E/Z* photoisomerization of **1**; b) UV/Vis spectra ( $1 \times 10^{-5} \text{ M}$ ) of 1-Z, 1-E and PSS<sub>365</sub> in toluene; c) *E/Z* photoisomerization of **2**; d) UV/Vis spectra ( $1 \times 10^{-5} \text{ M}$ ) of 2-Z, 2-E and PSS<sub>375</sub> in toluene.

of 79% *Z* ( $\Phi_{E\rightarrow Z}=12.0\pm 0.1\%$ ) and PSS<sub>375</sub> consisting of 88% *Z* ( $\Phi_{E\rightarrow Z}=10.7\pm 0.2\%$ ).<sup>[16]</sup>

The *E*→*Z* thermal relaxation rates of compounds **1** and **2** (Figures S19–20) were extrapolated to room temperature using Arrhenius and Eyring equations employing data measured in toluene at 333 K. In both cases, thermal relaxation half-lives of days were determined for **1** ( $\tau_{1/2}=14.1\pm 0.7$  days;  $k_{E\rightarrow Z}=(5.7\pm 0.3)\times 10^{-7}$  s<sup>-1</sup>) and **2** ( $\tau_{1/2}=24.2\pm 1.0$  days;  $k_{E\rightarrow Z}=(3.3\pm 0.1)\times 10^{-7}$  s<sup>-1</sup>). These half-lives are 4 orders of magnitude shorter than what is observed in the **parent** hydrazone ( $\tau_{1/2}=324$  years).<sup>[13]</sup> We previously discovered that having EDGs (–OMe or –NMe<sub>2</sub>) at the stator ring or EWG (–NO<sub>2</sub>) at the rotor ring will lead to rate acceleration. Our hypothesis is that these substituents impart a single-bond character on the C=N double bond, resulting in rotation around this bond as the major thermal relaxation pathway, as opposed to inversion at the imine nitrogen.<sup>[13]</sup> We speculate that the planarization-induced enhanced conjugation in the hydrazones, also imparts single-bond character on the imine bond (C=N) (Scheme 3), and thus lowers the activation barrier. Moreover, the *ford* region in **1** and **2** is more crowded in the *E* isomer (Scheme 3) relative to the **parent** system. We hypothesize that the resulting steric hindrance destabilizes the ground state thus decreasing the activation barrier further. We therefore attribute the day-scale half-lives observed in **1** and **2** to the combined effects of enhanced conjugation and the destabilization of the over-crowded ground state. As for the difference in rate between **1** and **2**, this effect may result from the resonance structure depicted in Scheme 3 being slightly less favorable in **2**, because of the electron withdrawing substituent.

In summary, we synthesized two new hydrazone switches that based on X-ray crystallography data are more planar than the parent system as a result of cyclization. Both molecules show red-shifted absorption bands for the *Z* and *E* isomers relative to their twisted counterparts. Moreover, the increased crowdedness at the *ford* region in the *E* form, along with the enhanced conjugation, bring about a 4 orders of magnitude acceleration in the thermal relaxation rates. This work sheds further light on the origins of the bistability of the newly developed hydrazone photoswitches, and ways to tune it. The structural similarity of **1** and **2** to the bioactive isochroman and/or its derivatives<sup>[17]</sup> also makes this class of hydrazone switches



**Scheme 3.** The proposed resonance structure in the cyclized hydrazone and the *ford* region are shown.

promising candidates for future photopharmacological applications.<sup>[6]</sup>

## Acknowledgements

We would like to acknowledge NSF program (CHE-1807428) for the generous support. We are grateful to Prof. Richard Staples (Michigan State University) for X-ray crystallography analysis.

**Keywords:** photochromism · hydrazone · red-shifted activation · isochroman · accelerated half-life

- [1] a) H. Durr, H. Bouas-Laurent, eds. *Photochromism: Molecules and Systems*, Elsevier Science, Amsterdam, **2003**; b) J. D. Harris, M. J. Moran, I. Aprahamian, *Proc. Natl. Acad. Sci. USA* **2018**, *115*, 9414–9422.
- [2] a) H. M. D. Bandara, S. C. Burdette, *Chem. Soc. Rev.* **2012**, *41*, 1809–1825; b) M. Hammerich, C. Schütt, C. Stähler, P. Lenters, F. Röhrich, R. Höppner, R. Herges, *J. Am. Chem. Soc.* **2016**, *138*, 13111–13114; c) C. Petermayer, S. Thumser, F. Kink, P. Mayer, H. Dube, *J. Am. Chem. Soc.* **2017**, *139*, 15060–15067; d) M. W. H. Hoorens, M. Medved, A. D. Laurent, M. Di Donato, S. Fanetti, L. Slappendel, M. Hilbers, B. L. Feringa, W. Jan Buma, W. Szymanski, *Nat. Commun.* **2019**, *10*, 2390.
- [3] a) Y. Yokoyama, *Chem. Rev.* **2000**, *100*, 1717–1739; b) M. Irie, T. Fukaminato, K. Matsuda, S. Kobatake, *Chem. Rev.* **2014**, *114*, 12174–12277; c) R. Klajn, *Chem. Soc. Rev.* **2014**, *43*, 148–184; d) J. R. Hemmer, S. O. Poelma, N. Treat, Z. A. Page, N. Dolinski, Y. J. Diaz, W. Tomlinson, K. D. Clark, J. P. Hooper, C. J. Hawker, J. Read de Alaniz, *J. Am. Chem. Soc.* **2016**, *138*, 13960–13966.
- [4] a) S. Erbas-Cakmak, D. A. Leigh, C. T. McTernan, A. L. Nussbaumer, *Chem. Rev.* **2015**, *115*, 10081–10206; b) S. Kassem, T. van Leeuwen, A. S. Lubbe, M. R. Wilson, B. L. Feringa, D. A. Leigh, *Chem. Soc. Rev.* **2017**, *46*, 2592–2621.
- [5] a) R. Klajn, J. F. Stoddart, B. A. Grzybowski, *Chem. Soc. Rev.* **2010**, *39*, 2203–2237; b) B. K. Pathem, S. A. Claridge, Y. B. Zheng, P. S. Weiss, *Annu. Rev. Phys. Chem.* **2013**, *64*, 605–630.
- [6] a) J. Broichhagen, J. A. Frank, D. Trauner, *Acc. Chem. Res.* **2015**, *48*, 1947–1960; b) M. M. Lerch, M. J. Hansen, G. M. van Dam, W. Szymanski, B. L. Feringa, *Angew. Chem.* **2016**, *128*, 11140–11163; *Angew. Chem. Int. Ed.* **2016**, *55*, 10978–10999.
- [7] a) H. A. Wegner, *Angew. Chem.* **2012**, *124*, 4869–4871; *Angew. Chem. Int. Ed.* **2012**, *51*, 4787–4788; b) D. Bléger, S. Hecht, *Angew. Chem.* **2015**, *127*, 11494–11506; *Angew. Chem. Int. Ed.* **2015**, *54*, 11338–11349.
- [8] a) C. E. Weston, R. D. Richardson, P. R. Haycock, A. J. P. White, M. J. Fuchter, *J. Am. Chem. Soc.* **2014**, *136*, 11878–11881; b) M. J. Moran, M. Magrini, D. M. Walba, I. Aprahamian, *J. Am. Chem. Soc.* **2018**, *140*, 13623–13627; c) A. Ryabchun, Q. Li, F. Lancia, I. Aprahamian, N. Katsonis, *J. Am. Chem. Soc.* **2019**, *141*, 1196–1200.
- [9] a) Y. Xiong, P. Rivera-Fuentes, E. Sezgin, A. V. Jentszsch, C. Eggeling, H. L. Anderson, *Org. Lett.* **2016**, *8*, 3666–3669; b) S. K. Patel, J. Cao, A. R. Lippert, *Nat. Commun.* **2017**, *8*, 15239; c) B. Shao, I. Aprahamian, *Chemphotochem*, **2019**, *3*, 361–364.
- [10] a) Y. Liao, *Acc. Chem. Res.* **2017**, *50*, 1956–1964; b) R. Kashihara, M. Morimoto, S. Ito, H. Miyasaka, M. Irie, *J. Am. Chem. Soc.* **2017**, *139*, 16498–16501; c) A. Gerwien, P. Mayer, H. Dube, *J. Am. Chem. Soc.* **2018**, *140*, 16442–16445.
- [11] a) S. M. Landge, I. Aprahamian, *J. Am. Chem. Soc.* **2009**, *131*, 18269–18271; b) X. Su, T. Lessing, I. Aprahamian, *Beilstein J. Org. Chem.* **2012**, *8*, 872–876; c) L. A. Tatum, X. Su, I. Aprahamian, *Acc. Chem. Res.* **2014**, *47*, 2141–2149; d) L. A. Tatum, J. T. Foy, I. Aprahamian, *J. Am. Chem. Soc.* **2014**, *136*, 17438–17441; e) Y. Yang, R. P. Hughes, I. Aprahamian, *J. Am. Chem. Soc.* **2014**, *136*, 13190–13193; f) J. T. Foy, D. Ray, I. Aprahamian, *Chem. Sci.* **2015**, *6*, 209–213; g) H. Qian, I. Aprahamian, *Chem. Commun.* **2015**, *51*, 11158–11161; h) S. Pramanik, I. Aprahamian, *J. Am. Chem. Soc.* **2016**, *138*, 15142–15145.
- [12] a) H. Qian, S. Pramanik, I. Aprahamian, *J. Am. Chem. Soc.* **2017**, *139*, 9140–9143; b) Q. Li, H. Qian, B. Shao, R. P. Hughes, I. Aprahamian, *J. Am. Chem. Soc.* **2018**, *140*, 11829–11835; c) B. Shao, M. Baroncini, H. Qian, L.

- Bussotti, M. Di Donato, A. Credi, I. Aprahamian, *J. Am. Chem. Soc.* **2018**, *140*, 12323–12327.
- [13] B. Shao, H. Qian, Q. Li, I. Aprahamian, *J. Am. Chem. Soc.* **2019**, *141*, 8364–8371.
- [14] C. T. Mbofana, S. J. Miller, *ACS Catal.* **2014**, *4*, 3671–3674.
- [15] Because of the different packing modes (Figure 2a another H-bond with slightly different values (2.70 Å, 127.19°) is also present.
- [16] Compound **1** also switches in PBS buffer (Figure S13) though less efficiently because of spectral overlap. Compound **2** on the other hand yields a different UV spectrum from what is observed in organic solvents and shows no signs of switching (Figure S14).
- [17] a) N. Khamthong, V. Rukachaisirikul, S. Phongpaichit, S. Preedanon, J. Sakayaroj, *Tetrahedron* **2012**, *68*, 8245–8250; b) R. Bai, X. Yang, Y. Zhu, Z. Zhou, W. Xie, H. Yao, J. Jiang, J. Liu, M. Shen, X. Wu, J. Xu, *Bioorg. Med. Chem.* **2012**, *20*, 6848–6855.

---

Manuscript received: November 18, 2019  
Revised manuscript received: January 15, 2020